

Magnetothermal study of the hybrid frustrated magnet $\text{Dy}_{2-x}\text{Tb}_x\text{Ti}_2\text{O}_7$

X. Ke,¹ D. V. West,² R. J. Cava,² and P. Schiffer¹¹*Department of Physics and Materials Research Institute, Pennsylvania State University, University Park, Pennsylvania 16802, USA*²*Department of Chemistry and Princeton Materials Institute, Princeton University, Princeton, New Jersey 08540, USA*

(Received 16 July 2009; revised manuscript received 23 September 2009; published 29 October 2009)

The two pyrochlore titanates $\text{Dy}_2\text{Ti}_2\text{O}_7$ and $\text{Tb}_2\text{Ti}_2\text{O}_7$ have low temperature magnetic states that result from geometrical frustration of the spin-spin interactions between neighboring rare-earth ions. $\text{Dy}_2\text{Ti}_2\text{O}_7$ is a canonical spin ice material, while the Tb moments in $\text{Tb}_2\text{Ti}_2\text{O}_7$ have a liquidlike cooperative paramagnetic state at low temperatures. We report magnetic and thermal properties of the hybrid rare-earth titanates, $\text{Dy}_{2-x}\text{Tb}_x\text{Ti}_2\text{O}_7$, with $0 \leq x \leq 2$. We find that both the magnetic and thermal properties of the materials are strongly affected by the mixture of the ions on the sites, and that the ground state of $\text{Dy}_{2-x}\text{Tb}_x\text{Ti}_2\text{O}_7$ is different from both spin ice and spin liquid, i.e., $\text{Dy}_{2-x}\text{Tb}_x\text{Ti}_2\text{O}_7$ is not a simple mixture of spin ice and spin liquid components or the corresponding nonmagnetic diluted species. The strongly altered low temperature behavior is presumably associated with the Dy-Tb spin interactions and the altered crystalline electric field, suggesting that such hybrid frustrated materials offer an alternative avenue through which to explore geometrical magnetic frustration.

DOI: [10.1103/PhysRevB.80.144426](https://doi.org/10.1103/PhysRevB.80.144426)

PACS number(s): 75.40.Cx, 75.40.Gb, 75.50.Lk

The study of the magnetic frustration associated with lattice geometry has attracted intense recent attention, due to the associated intriguing low temperature states.¹⁻⁴ Materials with the pyrochlore lattice, composed of corner-sharing tetrahedra, have been shown to display particularly rich low temperature behavior, and the rare-earth titanates ($\text{A}_2\text{Ti}_2\text{O}_7$) have been demonstrated to show a number of exotic magnetic states depending on the magnetic ions occupying on the rare-earth sites.⁴ In $\text{Ho}_2\text{Ti}_2\text{O}_7$ (Ref. 5) and $\text{Dy}_2\text{Ti}_2\text{O}_7$ (Ref. 6) for instance, the combination of Ising anisotropy and effective *ferromagnetic* exchange interactions results in a disordered spin state with two-in/two-out spin configuration on each tetrahedron, the so-called spin ice state.⁷ By contrast, $\text{Tb}_2\text{Ti}_2\text{O}_7$ appears to be a classical spin liquid or cooperative paramagnet at low temperatures, which has been attributed to the competition of Ising anisotropy, *antiferromagnetic* exchange interactions, dipolar interactions, and exchange coupling to non-nearest neighbors.^{8,9}

There have also been many reports on the derivative species of these rare-earth titanates, including stuffed¹⁰⁻¹⁵ compounds in which additional rare-earth ions are substituted for the Ti ions, and compounds in which nonmagnetic ion substitutions for the rare-earth ions are used to dilute the magnetic interactions.¹⁶⁻²¹ By contrast, there are few studies on hybrid rare-earth titanates, which consist of different rare-earth ions on the A sites. A brief recent report by Chang *et al.* on $\text{Ho}_{2-x}\text{Tb}_x\text{Ti}_2\text{O}_7$ ($x=0.5, 1.0, 1.5$) suggests that these hybrid compounds possess both spin ice and spin liquid characteristics in the ground state.²² Issues related to the nature of the interactions between different magnetic ions, the effect of the mixture of different rare-earth ions on the crystal field level schemes, and the effects on the ground state of the hybrid compounds have not been addressed. In this paper, we have carried out an extensive investigation of the $\text{Dy}_{2-x}\text{Tb}_x\text{Ti}_2\text{O}_7$ series over the full composition range between the two pure end members. Our data indicate that the magnetic interaction between Dy^{3+} and Tb^{3+} ions and the altered crystalline electric field in $\text{Dy}_{2-x}\text{Tb}_x\text{Ti}_2\text{O}_7$ result in a different low temperature magnetic state that is distinct from

the series end members and cannot simply be treated as a mixture of individual spin ice and spin liquid components. This is in striking contrast to as observed in the diluted materials wherein the characteristic of spin ice/spin liquid state preserves with nonmagnetic ions on the rare-earth sites.^{19,21}

Polycrystalline samples of $\text{Dy}_{2-x}\text{Tb}_x\text{Ti}_2\text{O}_7$ were synthesized using standard solid state synthesis techniques with $x=0, 0.2, 0.4, 1.0, 1.4, 1.8$, and 2. Starting materials for the synthesis were Dy_2O_3 , Tb_4O_7 , and TiO_2 . Samples with an appropriate mixture of starting materials were ground and then heated in air at 1400 °C with several intermittent heating and grinding steps. All samples were determined to be single phase pyrochlores by powder x-ray diffraction. The measured lattice constants increase continuously and linearly with increasing Tb concentration, suggesting a homogeneous solid solution Dy/Tb mixture. The magnetization M of each sample was measured using a Quantum Design superconducting quantum interference device (SQUID) magnetometer. The specific heat and ac magnetic susceptibility were determined using a Quantum Design Physical Property Measurement System (PPMS). Specific heat data were taken down to $T=0.7$ K with the ^3He option of the PPMS using a standard semiadiabatic heat pulse technique, and the samples measured were mixed with Ag powder and pressed into pellets to facilitate thermal equilibration. The real and imaginary parts of the ac susceptibility, χ' and χ'' , were determined using an excitation field of $H_{ac}=10$ Oe at frequencies spanning $f=100-10000$ Hz.

Temperature dependent dc magnetic susceptibility measurements show that there is no magnetic ordering or spin-glass-like transition occurring in any of the samples down to 1.8 K. Curie-Weiss fits to the data above 200 K give the effective temperature of -18 K for $\text{Tb}_2\text{Ti}_2\text{O}_7$, which is consistent with the previous reports,⁹ and -5 K for $\text{Dy}_2\text{Ti}_2\text{O}_7$. Both these values include significant contributions from the crystalline electric field, considering the first crystal field excitation of 18 K for $\text{Tb}_2\text{Ti}_2\text{O}_7$ (Ref. 9) and 200 K for $\text{Dy}_2\text{Ti}_2\text{O}_7$,²³ respectively. In order to be free of crystal field

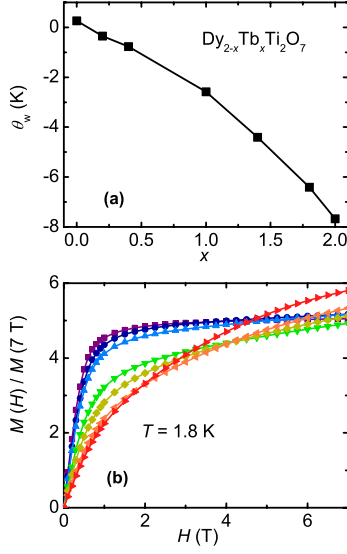


FIG. 1. (Color online) (a) Curie-Weiss temperature θ_W as a function of x for $\text{Dy}_{2-x}\text{Tb}_x\text{Ti}_2\text{O}_7$ derived from fits in the range of $T = 10\sim 20$ K. The measurement field is 100 Oe; (b) The magnetic field dependence of the magnetization M at $T = 1.8$ K for a series of $\text{Dy}_{2-x}\text{Tb}_x\text{Ti}_2\text{O}_7$ materials.

effects for the hybrid samples, we performed the Curie-Weiss fits for all samples in the temperature range $T = 10\sim 20$ K. The thus obtained Curie-Weiss temperatures θ_W are plotted in Fig. 1(a) as a function of Tb concentration. The slight positive θ_W for $\text{Dy}_2\text{Ti}_2\text{O}_7$ indicates effective ferromagnetic interaction for pure spin ice, while θ_W is about -8 K for $\text{Tb}_2\text{Ti}_2\text{O}_7$, which is close to the previous reported value⁹ and indicates antiferromagnetic spin interactions. The increasingly negative values of θ_W with increasing x represent the trend toward more antiferromagnetic effective exchange interaction with increasing Tb concentration.

Figure 1(b) shows the isothermal magnetization as a function of applied field, $M(H)$, at $T = 1.8$ K for $\text{Dy}_{2-x}\text{Tb}_x\text{Ti}_2\text{O}_7$ at several values of x . The magnetic moment of $\text{Dy}_2\text{Ti}_2\text{O}_7$ saturates with the magnetization value about $5.0 \mu_B/\text{Dy}$, half of the theoretical value, due to the single-ion anisotropy and powder averaging effect, while that of $\text{Tb}_2\text{Ti}_2\text{O}_7$ does not saturate up to $H = 7$ T. This unsaturated magnetization feature gets more obvious as Tb composition increases, as indicated by the decrease in the slope of the $M(H)$ curves at low fields, shown in Fig. 1(b). This is consistent with the increasing effective antiferromagnetic interaction shown in Fig. 1(a). Note that the magnetization at $H = 7$ T depends nonmonotonically on x , which can be presumably due to the magnetic interaction between Dy^{3+} and Tb^{3+} ions and the altered crystalline electric fields, as further discussed later.

Pure $\text{Dy}_2\text{Ti}_2\text{O}_7$ has previously been shown to display a frequency-dependent maximum in the ac susceptibility around 15 K, with the derived activation energy close to the first crystal field excitation.¹⁷ This feature has been associated with the single-ion relaxation process²⁴ and has also been observed in spin ice materials in which the rare-earth sublattice was diluted with nonmagnetic ions,^{17,19} where the associated spin relaxation time is affected by changes in the crystal field environment associated with the chemical pres-

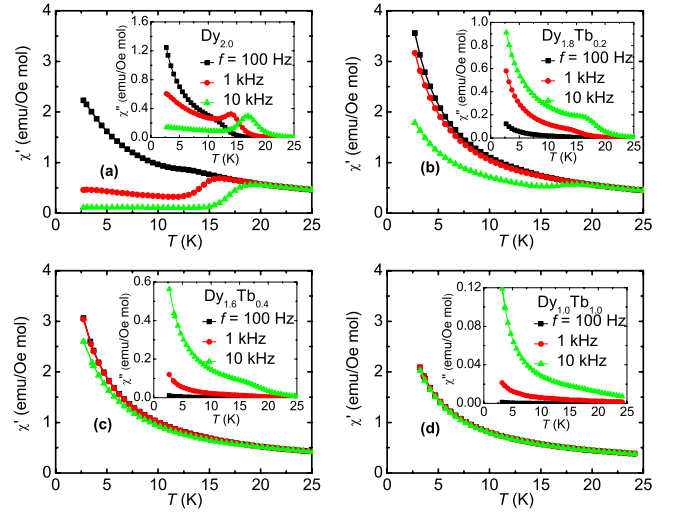


FIG. 2. (Color online) The measured ac magnetic susceptibility versus temperature for $\text{Dy}_{2-x}\text{Tb}_x\text{Ti}_2\text{O}_7$ for $x = 0$ (a), 0.2 (b), 0.4 (c), and 1.0 (d), at $f = 100, 1000$, and 10000 Hz. The main panels show the real part of ac susceptibility χ' and the insets show the imaginary part χ'' .

sure induced by substitution. In Fig. 2, we plot the temperature dependence of ac susceptibility as a function of temperature measured at zero field for $\text{Dy}_{2-x}\text{Tb}_x\text{Ti}_2\text{O}_7$ with $x = 0, 0.2, 0.4$, and 1.0 . Consistent with earlier studies,^{17,19} we observe maxima around 15 K for $\text{Dy}_2\text{Ti}_2\text{O}_7$, as shown in Fig. 2(a). This feature gets weaker for $\text{Dy}_{1.8}\text{Tb}_{0.2}\text{Ti}_2\text{O}_7$, and is barely observable, only in the imaginary part of the susceptibility, at $f = 10$ kHz for $\text{Dy}_{1.6}\text{Tb}_{0.4}\text{Ti}_2\text{O}_7$. The data appear to be completely frequency independent within our measurement frequency window for materials with larger x and no maxima are observed in $\text{Tb}_2\text{Ti}_2\text{O}_7$, as expected from earlier measurements.²⁵ These results indicate a faster spin relaxation process for materials with larger fraction of Tb and a dependence on Tb concentration that is quite different from the case of diluted spin ice materials mentioned above,^{17,19} where the spin relaxation time is a nonmonotonic function of dilution.

We now consider the thermodynamic behavior of $\text{Dy}_{2-x}\text{Tb}_x\text{Ti}_2\text{O}_7$. Figure 3(a) shows the temperature dependence of the zero-field magnetic heat capacity of the hybrid samples (after subtracting the phonon contribution to the heat capacity, using the scaled heat capacity of nonmagnetic $\text{Lu}_2\text{Ti}_2\text{O}_7$ as a reference, although the differences between the crystal field levels make a precise phonon background subtraction difficult). For pure $\text{Dy}_2\text{Ti}_2\text{O}_7$, we observe a peak around 1.2 K which corresponds to the spin ice freezing.^{7,19} On the other hand, for pure $\text{Tb}_2\text{Ti}_2\text{O}_7$, we find anomalies around 1.1 and 6 K, consistent with previous results.^{9,26} These two peaks have been ascribed to correlation effects on the single-ion ground state doublet and on the first excited doublet, respectively.⁹ The two peaks in $C(T)$ are discernable in our data for all $x > 0$, although the feature is broader and at higher temperature for small x . This is surprising due to the large differences of the first crystal field excitations for $\text{Tb}_2\text{Ti}_2\text{O}_7$ (~ 18 K) and $\text{Dy}_2\text{Ti}_2\text{O}_7$ (~ 200 K). It suggests that a small percentage substitution of Tb on the Dy sites

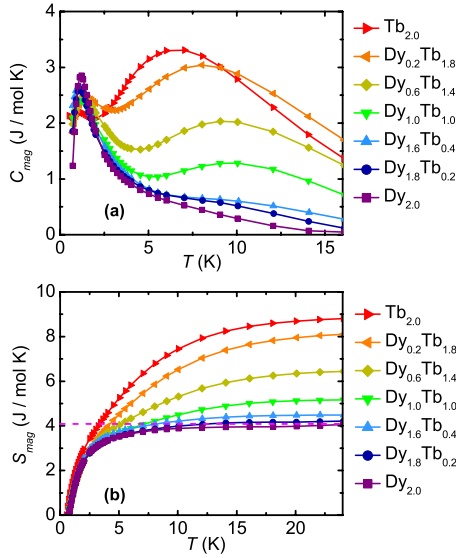


FIG. 3. (Color online) (a) The magnetic specific heat versus temperature for a series of $Dy_{2-x}Tb_xTi_2O_7$ materials at $H=0$ T. (b) Integrated magnetic entropy as a function of temperature of $Dy_{2-x}Tb_xTi_2O_7$ materials. The magenta dashed line represents the entropy for spin ice materials.

significantly alters the crystal field level, which sequentially affects the spin relaxation process, and is consistent with the changes we observe in the susceptibility discussed above. Surprisingly, there is no monotonic dependence of the position of the lower temperature anomalies on x , suggesting that the low temperature anomaly in the hybrid materials cannot be simply understood as resulting from either spin freezing or a simple crystal field effect.

In Fig. 3(b), we plot the integrated entropy as a function of temperature for the different samples. Note that we neglected the entropy contribution from Tb nuclear Schottky anomaly due to its small value above 0.7 K (where the calculated entropy is integrated from in our data).²⁶ $Dy_2Ti_2O_7$ shows a residual entropy of $1/2 \cdot R \ln 3/2$ (J/mol_{Dy} K) and it is consistent with previous reports.^{6,19} Without taking into account the entropy contribution below 0.7 K,²⁶ the entropy of $Tb_2Ti_2O_7$ is slightly less than $R \ln 4$, which recovers the entropy for the ground state doublets and first excited doublets.⁹ The entropy at high temperatures increases monotonically with increasing Tb concentration, mainly due to the increase in magnitude of the higher temperature anomaly as discussed above.

In order to gain insight into the spin-spin interactions between Dy^{3+} and Tb^{3+} ions and the crystal field levels in $Dy_{2-x}Tb_xTi_2O_7$, we compare the magnetization and the ac susceptibility of a $Dy_{2-x}Tb_xTi_2O_7$ sample with those obtained from the summation of two different sample combinations: $Dy_2Ti_2O_7$ with $Tb_2Ti_2O_7$ and $Dy_{2-x}Y_xTi_2O_7$ with $Tb_xY_{2-x}Ti_2O_7$. (The nonmagnetic diluted $Dy_{2-x}Y_xTi_2O_7$ and $Tb_xY_{2-x}Ti_2O_7$ materials were also synthesized using the solid state chemistry method described above and they also show the single phase pyrochlore structure.) In the discussion below, we focus on the $x=1$ case, but the conclusions appear to be qualitatively consistent for all values of x . Figure 4(a) shows the field dependence of magnetization at $T=1.8$ K for

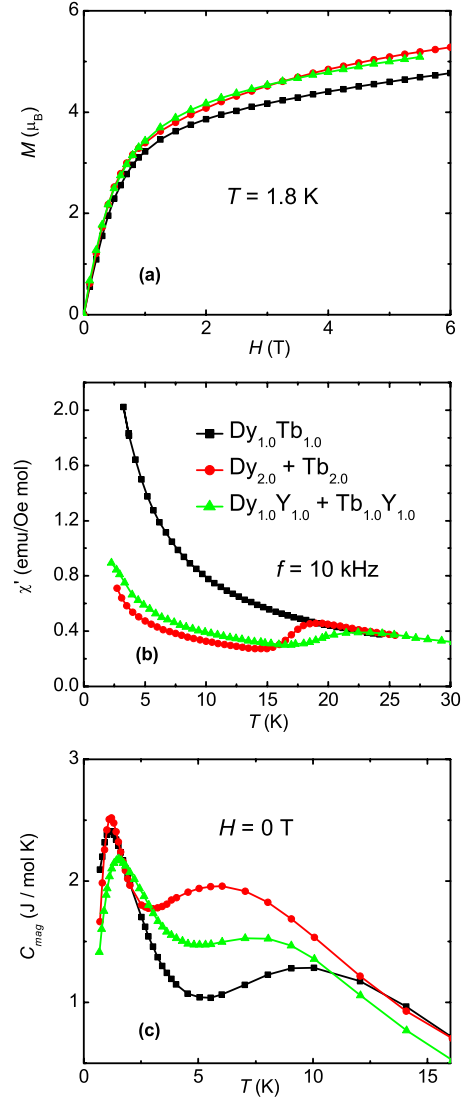


FIG. 4. (Color online) The magnetic field dependence of the magnetization M at $T=1.8$ K (a), temperature dependence of ac susceptibility χ' at $f=10$ kHz (b), and magnetic specific heat (c) of $Dy_{1.0}Tb_{1.0}Ti_2O_7$ (black), the summation of $Dy_2Ti_2O_7$ and $Tb_2Ti_2O_7$ (red), and the summation of $Dy_{1.0}Y_{1.0}Ti_2O_7$ and $Tb_{1.0}Y_{1.0}Ti_2O_7$ (green).

$Dy_{1.0}Tb_{1.0}Ti_2O_7$, the summation of $Dy_2Ti_2O_7$ and $Tb_2Ti_2O_7$, and the summation of $Dy_{1.0}Y_{1.0}Ti_2O_7$ and $Tb_{1.0}Y_{1.0}Ti_2O_7$ (normalized per formula unit in each case for consistency). We can see the $M(H)$ curves of the two summations overlap on each other, consistent with the fact that $M(H)$ curves for $Dy_{2-x}Y_xTi_2O_7$ and $Tb_xY_{2-x}Ti_2O_7$ materials vary only slightly with x . Interestingly, the $M(H)$ curve of $Dy_{1.0}Tb_{1.0}Ti_2O_7$ is distinct from these, showing a smaller magnetization. This is consistent with a strongly altered crystal field environment for the rare-earth ions in the $Dy_{2-x}Tb_xTi_2O_7$ compounds, or perhaps coupling between the Dy and Tb ions. Comparisons of the ac susceptibility of the above three sample configurations are shown in Fig. 4(b) with $f=10$ kHz at zero field. Note that the ac susceptibility of $Tb_{1.0}Y_{1.0}Ti_2O_7$ shows the canonical paramagnetic behavior as observed in $Tb_{2.0}Ti_2O_7$,²⁵ with no features. Thus, the maxima seen in

these two summation curves stems from the Dy materials only. This is quite different from the ac susceptibility measurement of the hybrid $\text{Dy}_{1.0}\text{Tb}_{1.0}\text{Ti}_2\text{O}_7$ material and provides additional evidence of the effect of the Dy-Tb spin interaction and the crystalline electric field. These results suggest that the hybrid $\text{Dy}_{2-x}\text{Tb}_x\text{Ti}_2\text{O}_7$ cannot be simply considered as a mixture of (diluted) spin ice and (diluted) spin liquid materials, but rather is a different magnetic system.

Finally, in Fig. 4(c) we compare the magnetic heat capacity of the above three sample configurations. The higher temperature anomaly of the two summation curves comes from the heat capacity of $\text{Tb}_2\text{Ti}_2\text{O}_7$ and $\text{Tb}_{1.0}\text{Y}_{1.0}\text{Ti}_2\text{O}_7$, respectively. The differences among these curves provides further confirmation that crystal field level of $\text{Dy}_{1.0}\text{Tb}_{1.0}\text{Ti}_2\text{O}_7$ is essentially different from that of the other two Tb compounds, and it again suggests that ground state of these hybrid compounds is more complicated than a simple mixture of the

characteristics of spin liquid and spin ice. Neutron scattering studies on $\text{Dy}_{2-x}\text{Tb}_x\text{Ti}_2\text{O}_7$ with isotopically enriched Dy would be desirable to address the crystal field level quantitatively and to determine the true ground state.

In summary, we have shown that the hybrid materials $\text{Dy}_{2-x}\text{Tb}_x\text{Ti}_2\text{O}_7$ exhibit magnetothermodynamic behavior distinct from both the (diluted) spin ice and (diluted) spin liquid materials. Such a difference may be attributed to the Dy-Tb interactions and the altered crystalline electric field. These results suggest the need for further exploration of geometrically frustrated magnets based on combinations of different magnetic ions on a single frustrated sublattice, since such hybrids have the potential to yield low temperature states not seen in systems with a single magnetic species.

We gratefully acknowledge financial support from NSF under Grants No. DMR-0701582 and No. DMR-0703095.

-
- ¹A. P. Ramirez, in *Handbook of Magnetic Materials*, edited by K. J. H. Buschow (Elsevier, Amsterdam, 2001), Vol. 13.
 - ²R. Moessner, *Can. J. Phys.* **79**, 1283 (2001).
 - ³H. T. Diep, *Frustrated Spin Systems* (World Scientific, Singapore, 2004).
 - ⁴J. E. Greedan, *J. Alloys Compd.* **408-412**, 444 (2006).
 - ⁵M. J. Harris, S. T. Bramwell, D. F. McMorrow, T. Zeiske, and K. W. Godfrey, *Phys. Rev. Lett.* **79**, 2554 (1997).
 - ⁶A. P. Ramirez, A. Hayashi, R. J. Cava, R. Siddharthan, and B. S. Shastry, *Nature (London)* **399**, 333 (1999).
 - ⁷S. T. Bramwell and M. J. P. Gingras, *Science* **294**, 1495 (2001).
 - ⁸J. S. Gardner, S. R. Dunsiger, B. D. Gaulin, M. J. P. Gingras, J. E. Greedan, R. F. Kiehl, M. D. Lumsden, W. A. MacFarlane, N. P. Raju, J. E. Sonier, I. Swainson, and Z. Tun, *Phys. Rev. Lett.* **82**, 1012 (1999).
 - ⁹M. J. P. Gingras, B. C. den Hertog, M. Faucher, J. S. Gardner, S. R. Dunsiger, L. J. Chang, B. D. Gaulin, N. P. Raju, and J. E. Greedan, *Phys. Rev. B* **62**, 6496 (2000).
 - ¹⁰G. C. Lau, R. S. Freitas, B. G. Ueland, B. D. Muegge, E. L. Duncan, P. Schiffer, and R. J. Cava, *Nat. Phys.* **2**, 249 (2006).
 - ¹¹H. D. Zhou, C. R. Wiebe, Y. J. Jo, L. Balicas, Y. Qiu, J. R. D. Copley, G. Ehlers, P. Fouquet, and J. S. Gardner, *J. Phys.: Condens. Matter* **19**, 342201 (2007).
 - ¹²G. C. Lau, R. S. Freitas, B. G. Ueland, M. L. Dahlberg, Q. Huang, H. W. Zandbergen, P. Schiffer, and R. J. Cava, *Phys. Rev. B* **76**, 054430 (2007).
 - ¹³B. G. Ueland, G. C. Lau, R. S. Freitas, J. Snyder, M. L. Dahlberg, B. D. Muegge, E. L. Duncan, R. J. Cava, and P. Schiffer, *Phys. Rev. B* **77**, 144412 (2008).
 - ¹⁴G. Ehlers, J. S. Gardner, Y. Qiu, P. Fouquet, C. R. Wiebe, L. Balicas, and H. D. Zhou, *Phys. Rev. B* **77**, 052404 (2008).
 - ¹⁵B. G. Ueland *et al.* (unpublished).
 - ¹⁶J. Snyder, J. S. Slusky, R. J. Cava, and P. Schiffer, *Nature (London)* **413**, 48 (2001).
 - ¹⁷J. Snyder, B. G. Ueland, A. Mizel, J. S. Slusky, H. Karunadasa, R. J. Cava, and P. Schiffer, *Phys. Rev. B* **70**, 184431 (2004).
 - ¹⁸G. Ehlers, J. S. Gardner, C. H. Booth, M. Daniel, K. C. Kam, A. K. Cheetham, D. Antonio, H. E. Brooks, A. L. Cornelius, S. T. Bramwell, J. Lago, W. Häußler, and N. Rosov, *Phys. Rev. B* **73**, 174429 (2006).
 - ¹⁹X. Ke, R. S. Freitas, B. G. Ueland, G. C. Lau, M. L. Dahlberg, R. J. Cava, R. Moessner, and P. Schiffer, *Phys. Rev. Lett.* **99**, 137203 (2007).
 - ²⁰G. Ehlers, E. Mamontov, M. Zamponi, A. Faraone, Y. Qiu, A. L. Cornelius, C. H. Booth, K. C. Kam, R. Le. Toquin, A. K. Cheetham, and J. S. Gardner, *J. Phys.: Condens. Matter* **20**, 235206 (2008).
 - ²¹A. Keren, J. S. Gardner, G. Ehlers, A. Fukaya, E. Segal, and Y. J. Uemura, *Phys. Rev. Lett.* **92**, 107204 (2004).
 - ²²L. J. Chang, H. Terashita, W. Schweika, Y. Y. Chen, and J. S. Gardner, *J. Magn. Magn. Mater.* **310**, 1293 (2007).
 - ²³S. Rosenkranz, A. P. Ramirez, A. Hayashi, R. J. Cava, R. Siddharthan, and B. S. Shastry, *J. Appl. Phys.* **87**, 5914 (2000).
 - ²⁴G. Ehlers, A. L. Cornelius, M. Orendac, M. Kajnakova, T. Fennell, S. T. Bramwell, and J. S. Gardner, *J. Phys.: Condens. Matter* **15**, L9 (2003).
 - ²⁵B. G. Ueland, G. C. Lau, R. J. Cava, J. R. O'Brien, and P. Schiffer, *Phys. Rev. Lett.* **96**, 027216 (2006).
 - ²⁶N. Hamaguchi, T. Matsushita, N. Wada, Y. Yasui, and M. Sato, *Phys. Rev. B* **69**, 132413 (2004).